

# INVESTIGATIONS ON RELATIONSHIP BETWEEN POROSITY AND ULTRASONIC ATTENUATION COEFFICIENT IN CFRP LAMINATES BASED ON RMVM

Shanshan DING<sup>1</sup>, Shijie JIN<sup>1</sup>, Zhongbing LUO<sup>1</sup>, Huan LIU<sup>1</sup>, Jun CHEN<sup>1</sup>, Li LIN<sup>1</sup>  
<sup>1</sup> NDT & E Laboratory, Dalian University of Technology, Dalian, China

**Abstract.** At present, the porosity of carbon fiber reinforced plastic (CFRP) is usually determined by measuring ultrasonic attenuation coefficient. The available detection models mainly focus on the ultrasonic scattering mechanism from regular voids, and pay little attention to the real random voids. However, some researches have demonstrated that the interaction between natural voids and ultrasonic beam is much more complicated than that of regular voids. Due to random and complex morphology of actual voids, it is extremely difficult to precisely describe the voids as well as their effects on ultrasonic scattering. In this paper, based on image processing technology and statistical methods, a real morphology void model (RMVM) was established for CFRP laminates. A series of photomicrograph with the porosity from 0.58% to 3.49% were simulated to investigate the relationship between porosity  $P$  and ultrasonic attenuation coefficient  $\alpha$ . Simulated results showed that the  $P$ - $\alpha$  scatter diagram presented a banded distribution, and the fluctuation range of attenuation coefficient enlarged with the increase of porosity. The non-unique corresponding relationship between  $P$  and  $\alpha$  was further verified by experiments. It is concluded that the complex void morphology affects the relationship between porosity and ultrasonic attenuation coefficient.

## 1. Introduction

Ultrasonic attenuation has been widely used to determine the porosity of carbon fiber reinforced plastics (CFRP) [1-3]. By measuring ultrasonic attenuation coefficient, the porosity was estimated in composite materials. In order to clarify ultrasonic scattering mechanism from voids in the composites, some ultrasonic scattering models have been established since 1970s. Martin [4, 5] firstly carried out a model of isotropic composites with regular spherical voids by assuming that the void sizes were uniform and the ultrasonic



scattering was independent of the void shape, etc. However, the theoretical calculation results were far less than experimental values. On this basis, Hale and Ashton [6] recognized that some assumptions proposed by Martin were unreasonable, for example, the scattering was independent of void shape. Then they presented a model with spherical and disc voids of distributed sizes. The bi-linear characteristic of curves between the ultrasonic attenuation coefficient and porosity showed a good consistency with experimental results, but the calculated values fit the experimental points well only for the lower detection frequency and porosity. Then, Hsu [7] developed a model of long cylindrical voids with elliptical cross-sections. The CFRP porosity was calculated using the “attenuation slop” algorithm based on spectral analysis. Although this theory was developed with unidirectional laminates, the cross-ply laminates showed a better similar attenuation-frequency relationship with experiment results. Birt and Smith [3] summarized the previous ultrasonic methods for porosity measurement, and concluded that the void morphology played an important role on the porosity detection. Thus, based on random medium theory and statistical principle, Lin et al [8-10] proposed a random void model (RVM). The spatial autocorrelation function and statistical parameters were used to describe the large-scale heterogeneity from the composite matrix and the small-scale heterogeneities of elastic fluctuations from random voids. Compared with the previous models (we named them “definite model”), RVM overcame the oversimplification on the void morphology [11, 12], in which the void shape was complex, the distribution was random and the size was non-uniform. The ultrasonic attenuation coefficients were in good agreement with experiment results for porosity below 1.5% and the deviation was significantly reduced beyond 1.5% porosity. Since RVM took into account of the complexity and randomness of the voids in the composite materials, which was essentially different from the definite models.

However, the void morphology of RVM, which was obtained by statistical data from microscopic observations of samples, was significantly affected by the quantity of observed voids. Besides, the void morphology determined by mathematical method was different with the natural voids. With the increase of porosity, there was still a difference between RVM simulated results and actual values of ultrasonic attenuation coefficient. To deeply understand ultrasonic scattering mechanism due to voids in composites, a real morphology void model (RMVM) based on RVM idea was further established with a great deal of CFRP photomicrographs, in which the void morphology was in conformity with the actual material. Then, the correlation between porosity  $P$  and ultrasonic attenuation coefficient  $\alpha_s$  was observed by numerical calculation for 441 RMVMs, and the validity of numerical calculation and modeling idea was verified by experiments. Furthermore, some RMVMs having different morphology with the same porosity or the same attenuation coefficient were performed to analyze the influence of void morphology on ultrasonic attenuation coefficient.

## 2. Principles

### 2.1 Ultrasonic scattering attenuation

The ultrasonic attenuation of composites containing voids mainly originates from the energy loss of resin together with fibers, and the scattering attenuation caused by voids. In this paper, the attenuation from fibers and resin is seen as a constant, and only the scattering attenuation caused by voids is to be considered.

According to the ratio of wavelength  $\lambda$  to mean diameter of scatterer  $D$  (Scatters are assumed to be spherical), ultrasonic scattering mechanism can be treated as the following three cases [13, 14]:

(1) Rayleigh scattering ( $\lambda \gg D$ ):  $\alpha(\lambda, D) = C_1 D^3 \lambda^{-4}$ ;

(2) stochastic scattering ( $\lambda \approx D$ ):  $\alpha(\lambda, D) = C_2 D \lambda^{-2}$ ;

(3) diffusion scattering ( $\lambda \ll D$ ):  $\alpha(\lambda, D) = C_3 D^{-1}$ ;

where  $\alpha$  is ultrasonic scattering attenuation coefficient;  $C_1$ ,  $C_2$  and  $C_3$  are the constants related to elastic parameters, density and ultrasonic velocity.

For typical CFRP laminates, ultrasonic wavelength is about 300~6000  $\mu\text{m}$  when the longitudinal wave velocity is 3000m/s under the conventional detection frequency (0.5~10MHz), while the void size ranges from tens to hundreds of micrometers. According to the ratio of the one-tenth of wavelength (30~600  $\mu\text{m}$ ) to void size, two kinds of mechanisms, Rayleigh scattering and stochastic scattering, are probably referred to CFRP specimens. Due to irregular shape, non-uniform sizes and random distribution, ultrasonic scattering mechanism of voids in composites is very complicated. Therefore, the precise calculation of ultrasonic scattering attenuation is difficult to be obtained directly using analytical method.

### 2.2 Modeling principles

As presented in Figure 1, the establishment of RMVM mainly consists of the following procedures after photomicrographs of CFRP samples were obtained. Firstly, the median filtering was used to blur the boundaries of fibers and resin in images, so that they could be treated as matrix [15]. Secondly, to effectively distinguished voids from matrix, the threshold was determined according to the gray histogram of filtered photo [16, 17]. It can be seen that the void morphology (as shown in Figure 1 (b)) is exactly the same as that of CFRP (Figure 1 (a)). Thirdly, the elastic parameters of matrix and voids were assigned, respectively.

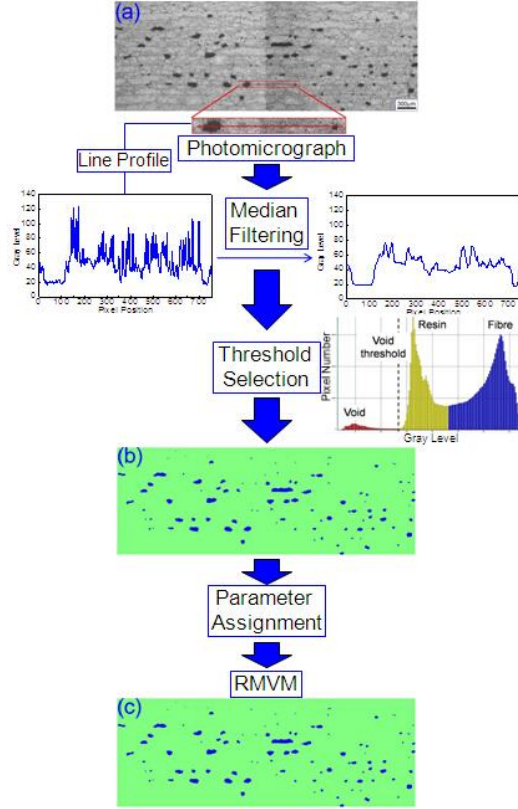


**Fig.1.** The establishment process of RMVM

### 2.3 Measuring principles of attenuation coefficient

The parts with uniform back echo amplitude in the C-scan image was selected, in which the attenuation coefficient was measured by ultrasonic echo immersion bottom reflection technique [18], and the experimental value  $\alpha_e$  (dB/mm) can be calculated as follow:

$$\alpha_e = \frac{10}{d} \left[ \lg \frac{A_{12}}{A_1} + 2 \lg(1 - R_1^2) \right] \quad (1)$$

where  $d$  is the sample thickness, and  $A_1$  and  $A_{12}$  represent the acoustic pressure of surface echoes from bottom with sample or not, respectively. Besides,  $R_1$  refers to the reflection coefficient at the interface between the sample and the water.

### 3. Numerical calculations

Based on the principle of asymptotic approximation, the 2D finite difference time domain method was used to simulate ultrasonic propagation. The area of RMVM shown in Fig 2 was  $4.44 \times 1.69 \text{mm}^2$ , and the simulated region was extended to avoid reflected waves from the left and right boundaries. Furthermore, the new bilateral boundaries were selected with longitudinal/shear mode fixed boundary. The absorbing boundary condition was set at the top so that the ultrasound cannot be reflected downward, while a free boundary was provided at the bottom. The probe was placed at the upper boundary of RMVM, and a Sine-Gauss

function was chosen as the pulse function, which was similar to the actual emission pulse. The other parameters were referred to [9].

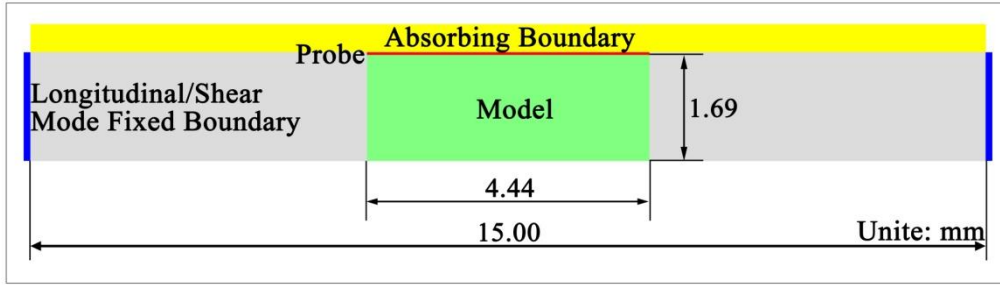


**Fig.2.** Schematic of calculating model

Employing the acoustic pressure of incident wave and reflected echo obtained by numerical simulation, the ultrasonic attenuation coefficient  $\alpha_s$  could be calculated according to equation (2):

$$\alpha_s = 10 \times \frac{1}{d} \lg \frac{p_0}{p} \quad (2)$$

where  $p_0$  and  $p$  were the acoustic pressure of incident wave and reflected wave, respectively.

## 4. Results of simulation and experiment

### 4.1 CFRP sample and testing condition

A series of 16-layered press molding unidirectional CFRP laminates were investigated, which were prepared by hand paste molding craft. The thickness and the fiber content were  $2 \pm 0.05\text{mm}$  and  $69 \pm 3\%$ , respectively. The CFRP laminates were scanned by the ultrasonic C-scan equipment with a focusing immersion probe (5 MHz centre frequency, 12mm diameter). According to the amplitudes of ultrasonic echoes, some uniform regions with the diameter of more than 6mm were selected as test areas.

The time-domain waveforms acquired from the selected regions were recorded to calculate  $\alpha_e$  by equation (1). Then, the CFRP laminates were cut and made into samples for metallographic experiment. The samples after grinding and polishing were shot to get photomicrographs for establishing RMVM. Finally, the porosity values of test areas were obtained, and the ultrasonic attenuation coefficients were calculated by equation (2).

### 4.2 Results of experiment and simulation

Taking 441 RMVMs with the porosity from 0.58% to 3.49% for simulation, attenuation coefficient versus porosity was shown in Figure 3. It could be seen that the ultrasonic attenuation coefficients gradually increased with porosity, and there was a non-unique corresponding relationship between them. For example, the porosity 1.55% corresponded to a range of attenuation coefficient 2.24~3.05dB/mm, while some samples with a same attenuation coefficient 2.60dB/mm had the porosity varying from 1.10% to 1.87%. All

calculated plots located in the banded region enclosed by two fitting lines,  $\alpha=0.83P+0.79$  and  $\alpha=1.46P+1.10$ . It could be seen that the fluctuation range of attenuation coefficient enlarged with the increase of porosity, and the largest difference was up to 1.77dB/mm.

At the same time, the experimental results of  $\alpha_e$  as the function of  $P$  were also plotted as shown in Figure 3. It can be seen that experiments and simulations were in the same banded region. It is verified that the non-unique relationship exists between porosity of CFRP and ultrasonic attenuation coefficient.

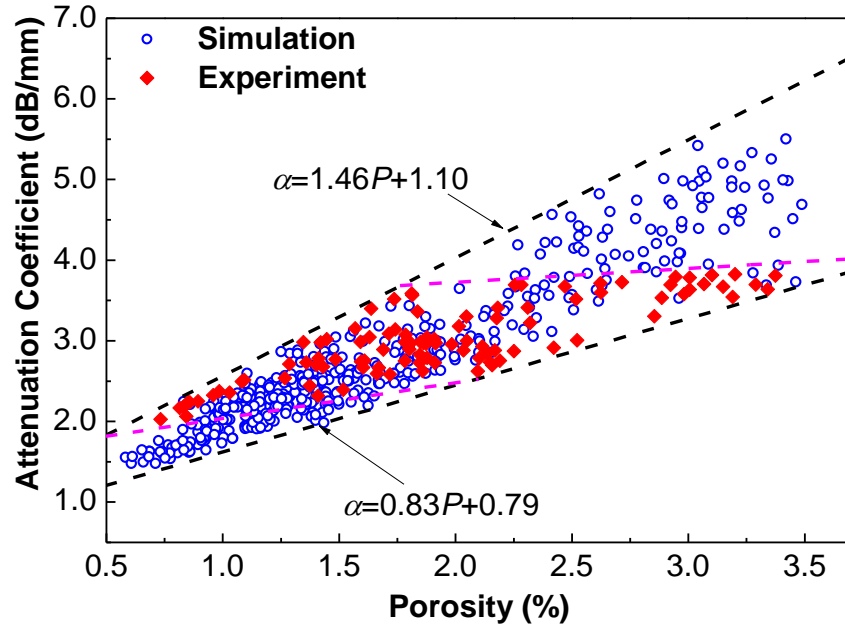


**Fig.3.** Ultrasonic attenuation coefficient versus porosity obtained by simulation (blue plots) and experiment (red plots)

Compared with experiments, it is also found that the simulation results of attenuation coefficient were smaller for low porosity, while significantly larger for high porosity. The reasons including without limitation were analyzed as follows: (1) the sample quantity and the porosity of RMVMs in the simulation were not the same as that of experiment, 441 RMVMs and 104 samples were used respectively; (2) the simulation results were obtained with two-dimensional models, while the actual samples and voids were three-dimensional structures.

#### 4.3 Analysis and discussions

The morphology of isolated dispersed voids in CFRP takes on complexity and randomness, such as the large quantities, various sizes, irregular shape, uncertain orientation and distribution. Affected by the factors mentioned above synthetically, the ultrasonic scattering mechanism for voids is significant complicated.

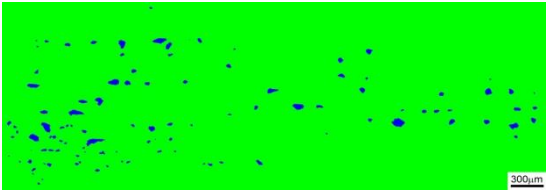
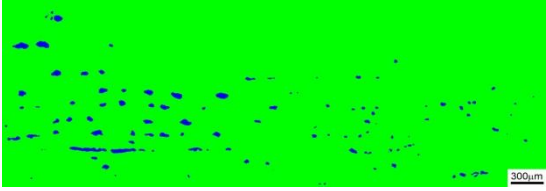
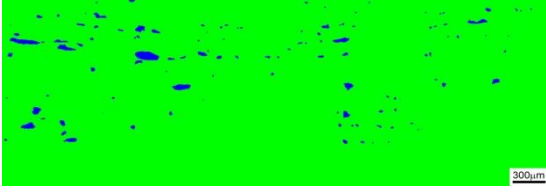
The validity of RMVM was proved by the consistency between experiment and simulation results. Based on RMVM, this paper attempted to quantitatively describe the complex morphology and analyze the influence of void morphology on the ultrasonic attenuation coefficient. The related statistical parameters of morphology included the

amounts of voids  $N$ , shape factor  $L^2/4\pi A$  (where  $L$  was the perimeter and  $A$  was the area), the horizontal size range of voids  $W_{min}\sim W_{max}$  and the average value  $W_m$ , etc.

(1) The same  $P$  (1.55%) with different  $\alpha_s$

Table 1 presents the morphology information of three RMVMs which had the same porosity and different  $\alpha_s$ . As shown,  $\alpha_s$ ,  $N$ ,  $W_{max}$  and  $L^2/4\pi A$  of 1# model are all minimums among the three RMVMs, which are 2.24dB/mm, 106, 152.7 $\mu\text{m}$  and 1.27, respectively. Especially, the shape factor (1.27) indicates that the void shape tend to be spherical. For 3# model, the attenuation coefficient (3.05dB/mm) is 36% higher than that of 1# model, and the  $N$  is up to 118. At the same time, the numbers of voids in 2# model and 3# model are close to each other, but there is a difference of 16% between the attenuation coefficients. Besides, compared with the other two RMVMs, 2# model has the largest  $W_{max}$  (304.2 $\mu\text{m}$ ) and shape factor (1.37).

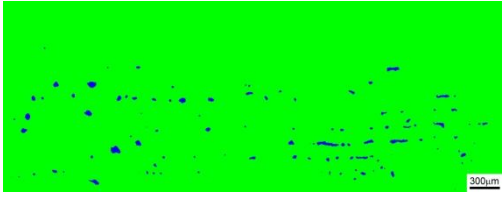
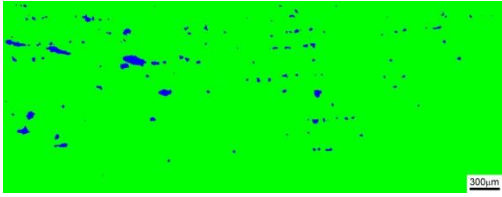
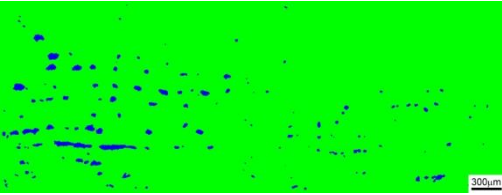
**Table.1** Three RMVMs with porosity of 1.55%

No.	RMVM	$\alpha_s$ (dB/mm)	$N$	$W_{min}\sim W_{max}$ $W_m$ ( $\mu\text{m}$ )	$L^2/4\pi A$
1#		2.24	106	7.4~152.7 42.6	1.27
2#		2.64	115	6.4~304.2 44.9	1.37
3#		3.05	118	7.4~250.2 41.3	1.32

(2) The same  $\alpha_s$  (2.60dB/mm) with different  $P$

Three RMVMs with the same  $\alpha_s$  are given in Table 2, and the porosity range 1.10%~1.87% means that the porosity of 3# model is 70% larger than that of 1# model. The varieties of  $L^2/4\pi A$  and  $W_m$  are not obvious with the increasing porosity, while  $N$  and  $W_{max}$  show an increasing trend. Furthermore, the shape, orientation and distribution of voids in models present significant differences and reveal the randomness of morphology.

**Table.2** Three RMVMs with ultrasonic attenuation coefficient of 2.60dB/mm

No.	RMVM	$P$ (%)	$N$	$W_{min} \sim W_{max}$ $W_m$ ( $\mu\text{m}$ )	$L^2/4\pi A$
1#		1.10	109	6.4~199.3 36.8	1.30
2#		1.48	125	7.4~226.9 36.2	1.28
3#		1.87	149	6.4~336.0 40.0	1.32

It is shown that the ultrasonic scattering attenuation due to voids in CFRP is affected not only by the porosity, but also by the void morphology, especially for high porosity. However, the ultrasonic scattering mechanism has still not been clarified thoroughly and needs to be investigated in further.

## 5. Conclusions

- (1) A RMVM for CFRP laminates containing voids was established based on the modeling idea of RVM, which can describe the nature void morphology and its elastic property;
- (2) For the porosity 0.58%~3.49%, both experiments and simulations verified the non-unique corresponding relationship between porosity and ultrasonic attenuation coefficient, and the validity of RMVM was confirmed by their consistency;
- (3) The non-unique corresponding relationship between  $P$  and  $\alpha$  is mainly caused by the diversity of random morphology of voids in composites.

## Acknowledgements

The project was supported by the National Basic Research Program of China (Grant No.2014CB046505) and the Natural Science Foundation of China (Grant No.51275075).

## References

- [1] Stone D E W, Clarke B. Ultrasonic attenuation as a measure of void content in carbon-fibre reinforced plastics. *Non-Destructive Testing* 1975; 8(3): 137-145.
- [2] Costa M L, Almeida S F M D, Rezende M C. The influence of porosity on the interlaminar shear strength of carbon/epoxy and carbon/bismaleimide fabric laminates. *Composites Science and Technology* 2001; 61(14): 2101 - 2108.
- [3] Birt E A, Smith R A. A review of NDE methods for porosity measurement in fibre-reinforced polymer composites. *Insight* 2004; 46(11): 681-686.
- [4] Martin B G. Ultrasonic wave propagation in fiber-reinforced solids containing voids. *Journal of Applied Physics* 1977; 48(8): 3368-3373.
- [5] Martin B G. Ultrasonic attenuation due to voids in fibre-reinforced plastics. *NDT International* 1976; 9(5): 242-246.
- [6] Hale J M, Ashton J N. Ultrasonic attenuation in voided fibre-reinforced plastics. *NDT International* 1988; 21(5): 321-326.
- [7] Nair S M, Hsu D K, Rose J H. Porosity estimation using the frequency dependence of the ultrasonic attenuation. *Journal of Nondestructive Evaluation* 1989; 8(1): 13-26.
- [8] Lin L, Ding S S, Chen J, Liang X Y, Li X M. Investigations on void morphology in CFRP composite materials and ultrasonic scattering attenuation based on a 2D random void model. *Proceedings of review of progress in quantitative nondestructive evaluation: Volume 31, 2012. AIP Publishing.*
- [9] Lin L, Zhang X, Chen J, Mu Y, Li X. A novel random void model and its application in predicting void content of composites based on ultrasonic attenuation coefficient. *Applied Physics A* 2011; 103(4): 1153-1157.
- [10] Lin L, Chen J, Zhang X, Li X. A novel 2-D random void model and its application in ultrasonically determined void content for composite materials. *NDT and E International* 2011; 44(3): 254 - 260.
- [11] McMillan A J. Material strength knock-down resulting from multiple randomly positioned voids. *Journal of Reinforced Plastics and Composites* 2012; 31(1): 13-28.
- [12] Kang T, Kim H H, Song S J, Kim H J. Characterization of fatigue damage of Al6061-T6 with ultrasound. *NDT & E International* 2012; 52(4): 51 - 56.
- [13] Smith R L. The effect of grain size distribution on the frequency dependence of the ultrasonic attenuation in polycrystalline materials. *Ultrasonics* 1982; 20(5): 211-214.
- [14] Reynolds W N, Smith R L. Ultrasonic wave attenuation spectra in steels. *Journal of Physics D: Applied Physics* 1984; 17: 109-116.
- [15] Liu H, Luo Z B, Ding S S, Lin L. Extracting void morphology of carbon fiber reinforced polymer by median filtering. *Sciencepaper Online* 2012.
- [16] Nakahata K, Schubert F, Kohler B. 3D imagebased simulation for ultrasonic wave propagation in heterogeneous and anisotropic materials. *AIP Conference Proceedings* 2011; 1335(1):51-58.
- [17] Kastner J, Plank B, Salaberger D, Sekelja J. Defect and porosity determination of fibre reinforced polymers by X-ray computed tomography. *Proceedings of the 2nd International Symposium on NDT in Aerospace, Hamburg, Germany, November 2010.*
- [18] Lin L, Luo M, Tian H T, Li X M, Guo G P. Experimental investigation on porosity of carbon fiber-reinforced composite using ultrasonic attenuation coefficient. *Proceedings of Proceedings World Conference on Nondestructive Testing, Shanghai, China, 2008.*